Eskelinen, Joona; Delikaris-Manias, Symeon; Gómez Bolaños, Javier; Hæggström, Edward; Pulkki, Ville

Beamforming with a volumetric array of massless laser spark sources—Application in reflection tracking

Published in:
Journal of the Acoustical Society of America

DOI:
10.1121/1.4920970

Published: 01/01/2015

Document Version
Publisher's PDF, also known as Version of record

Please cite the original version:
Eskelinen, J., Delikaris-Manias, S., Gómez Bolaños, J., Hæggström, E., & Pulkki, V. (2015). Beamforming with a volumetric array of massless laser spark sources—Application in reflection tracking. *Journal of the Acoustical Society of America*, *137*(6), EL389-EL395. https://doi.org/10.1121/1.4920970

Beamforming with a volumetric array of massless laser spark sources—Application in reflection tracking

Joona Eskelinen, Edward Hæggström, Symeon Delikaris-Manias, Javier Gómez Bolaños, and Ville Pulkki

Citation: The Journal of the Acoustical Society of America **137**, EL389 (2015); doi: 10.1121/1.4920970
View online: https://doi.org/10.1121/1.4920970
View Table of Contents: http://asa.scitation.org/toc/jas/137/6
Published by the Acoustical Society of America

Beamforming with a volumetric array of massless laser spark sources—Application in reflection tracking

Joona Eskelinen and Edward Hæggström
Department of Physics, University of Helsinki, P.O. Box 64, Helsinki FI-00014, Finland
joona.eskelinen@helsinki.fi, edward.haeggstrom@helsinki.fi

Symeon Delikaris-Manias, Javier Gómez Bolaños, and Ville Pulkki
Department of Signal Processing and Acoustics, Aalto University, P.O. Box 13000, Espoo FI-00076, Finland
symeon.delikaris-manias@aalto.fi, javier.gomez.bolanos@aalto.fi, ville.pulkki@aalto.fi

Abstract: A volumetric array of laser-induced air breakdown sparks is used to produce a directional and steerable acoustic source. The laser breakdown array element is broadband, point-like, and massless. It produces an impulse-like waveform in midair, thus generating accurate spatio-temporal information for acoustic beamforming. A laser-spark scanning setup and the concept of a massless steerable source are presented and evaluated with a cubic array by using an off-line far field delay-and-sum beamforming method. This virtual acoustic array with minimal source influence can, for instance, produce narrow transmission beams to obtain localized and directional impulse response information by reflection tracking.

[JM]
Date Received: December 19, 2014 **Date Accepted:** April 29, 2015

1. Introduction

A volumetric array refers to a beamforming array where the elements are positioned inside a volume, either by a physical array configuration or by synthesizing a virtual array from several positions of an element. Such arrays have been used in many fields, including antennas[1] and acoustics.[2] For acoustic applications, a volumetric array enables full three-dimensional (3D) steering of the source or receiver for directional analysis of the sound field, for instance, to obtain localized impulse response information. Ideally, the array would produce a highly directional beam without influencing the sound field. The preferred array element for such application should be point-like and omnidirectional, to permit using all the elements without shadowing. Most 3D source beamforming applications use spherical loudspeaker arrays,[3] where the elements are positioned on the surface of a sphere. Loudspeaker use for volumetric arrays is limited due to shadowing between the elements. Moreover, the speaker elements are directional which complicates their use in virtual arrays.

Laser induced breakdown (LIB) in air provides a point-like, repeatable, impulsive, and omnidirectional source with high peak pressure levels.[4] These characteristics make it a potential source for virtual acoustic beamforming. The LIB is generated by focusing the beam of a pulsed laser into a sufficiently small spot to exceed the optical intensity threshold for plasma production. After the breakdown is initiated the plasma expands with supersonic velocity and generates a shock-wave.[5] The propagation velocity of the shock-wave is determined by the energy released in the breakdown. For instance, with mJ-range laser pulse energy the shock-wave rapidly attenuates to a sonic wave and at room scale (>1 m) acoustics the initial velocity increase is not detectable.[4]

The LIB spark itself does not cause substantial reflections since the duration of dense plasma expansion and shock-wave generation is short. With 150–300 mJ pulse energy, the shock-wave is already decoupled from the plasma at 1 μs after the spark initiation and after 50 μs the plasma has cooled to 2000 K.[6] The focusing optics for LIB may cause reflections, which can be minimized by focusing as far as possible and by increasing the laser intensity. If necessary, the focal distance can be further increased by expanding the beam before focusing[7] to decrease the focal spot size. The broadband and point-like nature of LIB provides high temporal resolution for adjusting the phase delays in beamforming. This holds especially in the high frequency domain, where the ratio between wavelength and temporal resolution is small. Moreover, the LIB source can be arbitrarily positioned, for instance, inside small spaces or close to object edges (e.g., inside a small tube).[7]

The laser parameters (wavelength, pulse duration, pulse energy, and focusing) and air impurities affect the breakdown process, hence influencing the acoustic characteristics and the stability of the spark source. With nanosecond time-scale laser pulses the breakdown initiation is not deterministic and the individual LIB sparks can differ in amplitude and location.[8] However, the repeatability of LIB produced by a 5–8 ns and 200–1000 mJ neodymium-doped yttrium aluminum garnet (Nd:YAG) laser pulse suffices for acoustic applications.[4,7] Moreover, since most LIB applications would be off-line, averaging can be used to improve the signal-to-noise ratio (SNR).

Several LIB sparks can be used to form a volumetric array (i.e., a matrix) in midair by moving the focusing point of the laser. Since LIB is produced in midair, there are no physical constraints to the spatial configuration of the source matrix. The matrix can have arbitrary size and shape that can be tailored, e.g., to optimize the aperture for a specific application. However, practical limitations may arise from the optical scanning setup. Regardless of array configuration, the masslessness and omnidirectionality of the LIB enables directing sound with an unperturbed full 3D field-of-view. Since the beamforming is done on the transmit side, reflection tracking or directional impulse response measurements can be done with a single small-footprint omnidirectional receiver. This approach minimizes the receiver influence, in addition to the influence of the source.

The aim of this work is to produce a LIB matrix to study its beamforming capabilities. As a proof-of-concept, reflections from a large object and from the floor are tracked by scanning a beam across them.

2. Methods and setup

The massless matrix beamforming method consisted of producing a laser spark matrix, spark-by-spark, in midair with a pulsed laser and recording the response of the entire matrix with a single stationary microphone. The spark positions, which are input to the beamformer algorithm, were determined by four additional microphones. A time domain far field delay-and-sum (DAS) method was employed to produce a beam along a chosen direction from the matrix center. The DAS was selected due to its simplicity to demonstrate the capability for impulse beamforming. The beamforming was done off-line after the measurements. Each of these processes are described in the Secs. 2.1–2.3.

2.1 LIB generation and scanning

The LIB source was produced by focusing the output of a 415 mJ Nd:YAG pulsed laser (CFR400, 1064 nm/8 ns/4.5 mrad divergence, Quantel-Laser, France) with a 75 mm focal distance lens (LA1608-B, Thorlabs, Newton, NJ). The laser head was positioned horizontally, while the beam was tilted 90°, towards the ceiling, with a mirror (NB1-K13, Thorlabs, Newton, NJ) placed 96 cm in front of the laser head [see Fig. 1(a)]. The focusing lens was positioned on top of the mirror, producing the focal point 17.5 cm above it. The laser spark position was scanned semi-automatically by moving the laser head and the focusing lens attached to it. The laser head resided on a

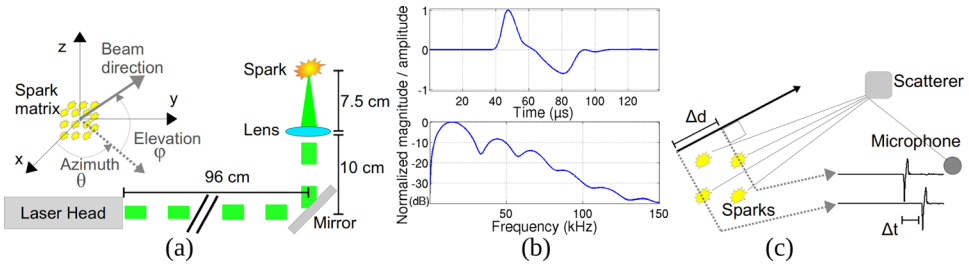

Fig. 1. (Color online) (a) Setup and the coordinate system. (b) Normalized LIB impulse (top) and its bandwidth (bottom). (c) A visualization of the DAS reflection tracking concept.

z-direction scannable lab-jack that was anchored to an automated rotation table (ET250-3D, Outline, Italy). The laser-head and lab-jack ensemble was integrated into a manually movable rack with guided movement along the floor. All measurements were done in a 6.35 m × 5.58 m × 2.72 m room.

2.2 Signal recording and conditioning

The position of each spark was determined using multilateration by measuring the time-of-flight to four 1/4 in. microphones (type 46BF, G.R.A.S., Denmark) positioned outside the spark matrix volume ([139, 144, 112, 57] cm from the matrix center). The matrix center was 140 cm above the floor. For each matrix position 51 individual sparks were recorded and averaged using 2 Hz pulse repetition frequency. A total of 216 laser spark positions were recorded forming a $6 \times 6 \times 6$ matrix with 8 mm spacing and $4 \times 4 \times 4\,\text{cm}^3$ volume. The cubic spark array was chosen to facilitate scanning and the array configuration was a compromise between locality, spatial aliasing, and number of the sparks.

The receiver was a 1/8 in. pressure microphone (type 40DP, G.R.A.S., Denmark) placed 140 cm from the center of the source matrix and 140 cm above the floor. The microphone is omnidirectional within audible frequencies, implying a minimal influence on the reflection tracking tests. The receiver signal was input to a signal conditioner (type 12AG, G.R.A.S., Denmark) and digitized with 400 kHz sampling rate using a data acquisition device (NI PXI-5922, National Instruments, Austin, TX). The setup was controlled with a computer running LabView (National Instruments, Austin, TX). To improve the temporal resolution and to increase the sampling points within the duration of the impulse the signal was up-sampled to 4 MHz sampling rate. Figure 1(b) shows a LIB impulse and its bandwidth at 140 cm from the source. The impulse has large bandwidth and short duration. However, the shape and duration limits its low frequency content.

2.3 Beam synthesis and signal processing

The beamforming consisted of using the measured spark locations to calculate an individual delay for each spark corresponding to the chosen beam direction [see Fig. 1(c)]. The beam direction was relative to the center of the LIB matrix that was determined as the mean of all matrix spark positions. The beam synthesis employed the equation

$$R(t,\theta,\varphi) = \frac{1}{N}\sum_{n=1}^{N} S_n\left(\frac{d_{nF} - D_F}{c} + t\right), \tag{1}$$

where R represents the signal at the recording position, N is the total spark position count ($N = 216$), n is the number of the current spark, S_n is the recorded signal of the nth spark, d_{nF} is the distance from the nth spark to the far field focusing point at the given azimuth (θ) and elevation (φ) direction, D_F is the distance from the matrix center to the far-field focusing point, c is the sound velocity (344 m/s), and t the time instant.

The delays were calculated using the far-field assumption, meaning that only delays respective to the beam direction [Δt, Fig. 1(c)] were taken into account. In practice this was done by choosing D_F sufficiently large. The maximum distance of a spark relative to the matrix center is 3.5 cm. At 140 cm distance from the source the difference between accurate delays and the far-field assumption is negligible (0.03%).

Signal deconvolution was also investigated to increase the bandwidth of the beam. This was done before the DAS. The deconvolution was performed using a windowed direct sound of the first spark as a reference and was truncated to 150 kHz. The DAS plus deconvolution process is similar to using a frequency domain beamformer in which the DAS produces the phase weights while the deconvolution gives the amplitude weights.

2.4 Beam evaluation

To evaluate the beamformer performance the beam was rotated 360° with 0.1° angular resolution in both the azimuthal and elevation planes. The signal was synthesized at the location of the measurement microphone (140 cm distance, 0° elevation, and 79° azimuth). Angular polar plots of the beam were produced by taking the maximum of the first arriving anechoic impulse inside a 400 μs time window. The spectral beam profiles were produced by calculating the magnitude of the Fourier transform for the same windowed signal for each beam angle.

2.5 Reflection tracking

A reflection tracking test was done for an object (H57 cm × W36 cm × D35 cm loudspeaker with a rough aluminum surface) that was positioned 15 cm below and +55° (azimuth) off a line between the matrix and the recording microphone. A beam was scanned across the object in 0.1° steps along the azimuth direction and the maximum amplitude of the reflection was determined from a 400 μs wide window. The same tracking process was repeated in the elevation direction for a floor (parquet) reflection between the matrix and the recording microphone (at azimuth 78°).

3. Results

Beamformer results for direct sound are presented in Fig. 2. Figure 2(a) shows the temporal response of an azimuthal scan across the recording microphone and the first arriving reflections. The time domain beam [Fig. 2(b)] has a main-lobe width (−6 dB) of 19°, at 140 cm distance, and reduces to 7.4° after the deconvolution. The result is similar in both planes. The frequency response at the beam center [at 78°, Fig. 2(c)] is similar to the response of the individual sparks [Fig. 1(b)], and is almost

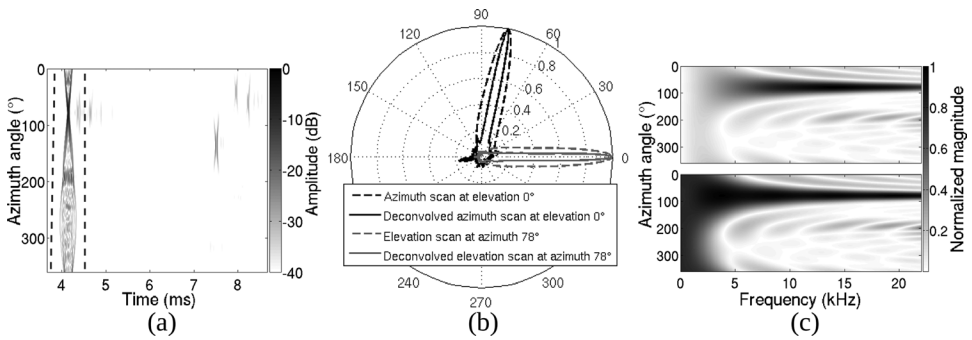

Fig. 2. Beam synthesis performance. (a) Azimuthal angular scan at elevation 0° showing the direct sound and first reflections. The dotted lines depict the region for angular analysis. (b) Polar plot presenting the angular maximum amplitude of the direct impulse scanned across the receiver in both azimuth and elevation planes and for both normal and deconvolved signals. (c) Frequency response for the windowed direct sound for both normal (top) and deconvolved (bottom) signals from the azimuthal scan.

omnidirectional at low frequencies. The reflection tracking results are presented in Fig. 3. Both the tracked object and the floor are reconstructed at correct angular locations [Fig. 3(a), dashed circle]. Reflections from objects in the ceiling and from a wall are also noticeable. The angular width of the deconvolved reflection from the object and floor are 8.6° and 13.2° [Fig. 3(b)], respectively. The "sidelobe" that is evident in the floor reflection [Fig. 3(b) at 60°] is caused by a reflection from an object in the ceiling.

4. Discussion

The results indicate the potential of using LIB for massless virtual beamforming. The frequency spectrum of the beam is similar to that of the individual sparks at a given distance and the impulse characteristics are adequately maintained in the beam, making the method feasible for directional and temporally resolved impulse response measurements. This is supported by the short duration of the pulse and the narrow width of the beam.

The spectrum of the beam extends beyond audible frequencies, while the peak frequency at 1–2 m distance from the source is 14–15 kHz. For reflection tracking a large bandwidth is preferable since it increases the spatio-temporal accuracy. For impulse response analysis the beam can be filtered to the desired bandwidth. The SNR is sufficient to enable deconvolution, which can be used to increase the beam bandwidth to produce even narrower beams. For instance, using the 150 kHz deconvolution the beam width was decreased from 19° to 7.4°.

The DAS beamformer performance depends on accurate temporal alignment of the pulses along the beam direction. With large bandwidth and short duration pulses the beamforming delays need to be accurate. A characteristic of the 3D DAS beamformer utilizing omnidirectional short impulses is that the impulses propagating outside the beam produce background noise. Due to short impulse duration there is negligible negative phase cancellation but the impulses can coherently sum up at specific delays. This effect is noticeable, e.g., between the dashed lines in Fig. 2(a).

The cubic matrix generates distinguishable lobes in the beam due to coherent summing of the spark lines along the matrix diagonals [Fig. 2(b), at 185°]. This effect could be reduced by using a pseudorandom configuration for the spark positions.[1,2] Moreover, a spherical matrix would be preferred since it produces a constant aperture for all angles, provided that the number of sparks is sufficient and that they are positioned uniformly (on a surface) or randomly (in a volume). Spatial amplitude weights can also be applied to the sparks to smooth the angular performance. The compact size of the measured matrix provides source locality but reduces the low frequency

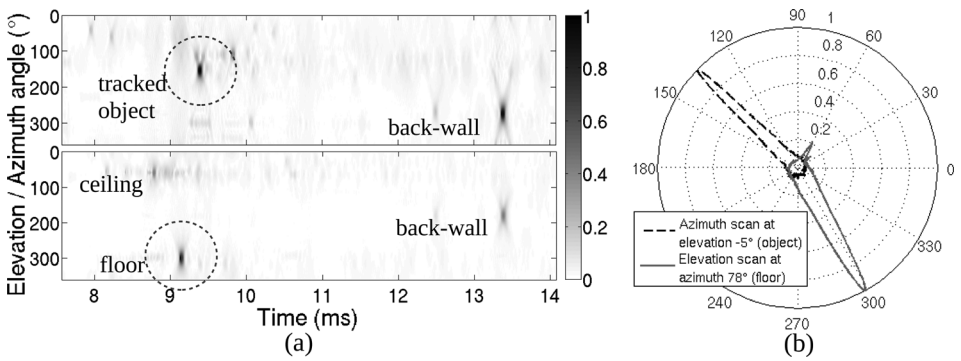

Fig. 3. Reflection tracking results. (a) Temporal reflection amplitude reconstructions of an azimuth beam scan at −5° (355°) elevation (top) and an elevation beam scan at azimuth 78° (bottom). The reflection from the tracked object and from the floor are marked with a dashed circle. To facilitate visualization of the reflections the amplitude envelope is plotted in linear scale and without deconvolution. (b) Angular polar plot of the maximum reflection amplitude (deconvolved) for both the object and the floor.

directivity for beam synthesis. A larger aperture would however reduce the locality and point-like characteristics and thus impair the accuracy of the far field reflection tracking. Moreover, for a certain shape and size of the matrix a high number of sparks increases beam quality but simultaneously increases the scanning time.

The accuracy of spark location estimates can affect the beam performance. The average standard deviation of all the averaged sparks in a single position was 0.5 mm. This includes the fluctuation of the spark position, sampling accuracy, and multilateration errors. Moreover, the scanning setup was designed for large matrices and the positioning is not accurate within sub-millimeter range. However, the matrix position errors or possible sound velocity inaccuracy had no significant effect, since the maximum beam amplitudes were 89.2% and 97.6% compared to ideal superposition amplitude of all the individual sparks (with and without deconvolution, respectively). This finding was also confirmed by testing the beamformer with small changes in the positions and in the reconstruction velocity. For small matrices the scanning could be improved by using, e.g., a xyz-translation stage, steerable mirror or a spatial light modulator.[9] With accurate scanning, provided that the spark repeatability is sufficient, the spark position monitoring would not be needed.

The reflection tracking results validate the beamformer performance. Individual reflections are evident and their amplitude changes within the angular beam scanning. The reflection from the tracked object exhibits a maximum at the correct angular location. The reflection from the floor also occurs at the correct angular location and has wider angular width than the object. The floor is a flat target, so a wider response compared to that from the finite size object is expected. Back-wall and ceiling reflections are produced at correct locations, thus supporting the 3D beamforming capability of the matrix. These results indicate that the proposed kind of reflection tracking by source steering is feasible with minimal source influence and with a single receiver microphone.

Due to point source and receiver characteristics and by assuming reciprocity the LIB matrix could be considered to be a massless receiver matrix whereas the microphone would be an omnidirectional point source. If the matrix is produced at the desired receiver location, the spark beamformer could then be used for direction-of-arrival detection. The massless and point-like nature of the LIB opens up possibilities for novel diffraction studies since the source can be arbitrarily positioned, e.g., close to objects where a physical speaker would not fit. In addition to room-scale, the LIB matrix could be utilized in small-space applications, since the matrix can be scaled down, and at short distances the bandwidth extends to MHz frequencies.

5. Conclusions

A volumetric array of laser induced air breakdown sparks was used for acoustic beamforming. The massless beamforming matrix can be produced in midair with minimal source influence. The impulse characteristics and large bandwidth of the LIB induced impulse enables accurate timing and distance information for beamforming. The directional beams can be used for reflection tracking to obtain local impulse response information.

Acknowledgments

This work was supported by The Academy of Finland (Project No. 121252), the Aalto ELEC doctoral school, and by the European Research Council under the European Community's Seventh Framework Programme (FP7/2007-2013)/ERC Grant No. 240453.

References and links

[1]A. Tennant and A. F. Fray, "A 64 element broad band volumetric array antenna," in *IEEE Antennas and Propagation Society International Symposium 1998* (1998), Vol. 3, pp. 1417–1420.

[2]J. M. Rigelsford and A. Tennant, "A 64 element acoustic volumetric array," Appl. Acoust. **61**, 469–475 (2000).

[3]B. Rafaely, "Spherical loudspeaker array for local active control of sound," J. Acoust. Soc. Am. **125**, 3006–3017 (2009).
[4]J. Gómez Bolaños, J. Eskelinen, S. Delikaris-Manias, V. Pulkki, and E. Hæggström, "Laser-induced acoustic point source for accurate impulse response measurements within the audible bandwidth," J. Acoust. Soc. Am. **135**, EL298–EL303 (2014).
[5]Q. Qin and K. Attenborough, "Characteristics and application of laser-generated acoustic shock waves in air," Appl. Acoust. **65**, 325–340 (2004).
[6]H. Sobral, M. Villagrán-Muniz, R. Navarro-González, and A. C. Raga, "Temporal evolution of the shock wave and hot core air in laser induced plasma," Appl. Phys. Lett. **77**, 3158–3160 (2000).
[7]N. Hosoya, M. Nagata, and I. Kajiwara, "Acoustic testing in a very small space based on a point sound source generated by laser-induced breakdown: Stabilization of plasma formation," J. Sound Vib. **332**, 4572–4583 (2013).
[8]Y. L. Chen, J. Lewis, and C. Parigger, "Spatial and temporal profiles of pulsed laser-induced air plasma emissions," J. Quant. Spectrosc. Radiat. Transf. **67**, 91–103 (2000).
[9]E. Lyon, Z. Kuang, H. Cheng, V. Page, T. Shenton, and G. Dearden, "Multi-point laser spark generation for internal combustion engines using a spatial light modulator," J. Phys. D: Appl. Phys. **47**, 475501 (2014).